Theoretical Population Biology 163 (2025) 1–12

Contents lists available at ScienceDirect

Theoretical Population Biology

journal homepage: www.elsevier.com/locate/tpb

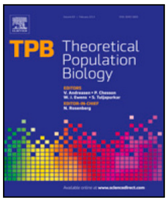

A mathematical framework for time-variant multi-state kinship modelling

Joe W.B. Butterick *, Peter W.F. Smith, Jakub Bijak, Jason Hilton

Department of Social Statistics and Demography, University of Southampton, Southampton SO17 1BJ, United Kingdom

ARTICLE INFO

Dataset link: https://github.com/ButterickJoe/Simulation_Age_Stage_Kinship

Keywords:
Mathematical demography
Kinship
Matrix projections
Markov process
Age×stage-structured populations

ABSTRACT

Recent research on kinship modelling in demography has extended age-structured models (i) to include additional characteristics, or "stages" (multi-state kinship), and (ii) to time-variant situations. A wide variety of population structures can affect kinship networks. However, only one prior model has comprehensively considered such effects, and under specific assumptions relating to the nature of individuals' stages. As such, the leading multi-state framework for kin is theoretically limited in scope, and moreover, has yet to be implemented under time-variant demographic rates. Generalising kinship models to encompass arbitrary population characteristics and extending them to time-dependent processes remain open challenges in demography.

This research proposes a methodology to extend multi-state kinship. We present a model which theoretically accounts for any stage, both in time-variant and time-invariant environments. Drawing from Markov processes, a concise mathematical alternative to existing theory is developed.

The benefits of our model are illustrated by an application where we define stages as spatial locations, exemplified by clusters of local authority districts (LADs) in England and Wales. Our results elucidate how spatial distribution – a demographic characteristic ubiquitous across (and between) societies – can affect an individual's network of relatives.

1. Introduction

Mathematical demographic models of kinship stem from the influential papers of Goodman et al., 1974 and Pullum, 1982. However, as a recent commentary in the pages of this journal has noted (Pavard and Coste, 2020), in the decades following the publication of Goodman et al.'s paper (Goodman et al., 1974), with the exception of Goldman (1978) and Coresh and Goldman (1988), few other authors invested much energy in the mathematical study of kinship. In recent years, there has been something of a resurgence in the area, including notable theoretical papers by Coste et al. (2021) and Caswell (2019b, 2020), Caswell and Song (2021), Caswell (2022). In Caswell (2019b), a one-sex age-structured population model subject to time-invariant demographic rates is proposed. A system of matrix projections are derived: one for each kin of some typical population member (termed Focal henceforth). Subsequent to its inception, this matrix-based framework has been extended to time-variant demographic rates (Caswell and Song, 2021), and age×stage (multi-state) structured populations (Caswell, 2020). Stage in this context refers to any population characteristic for which individuals can transition in and out of. Developing the theoretical synthesis of Caswell (2020) to cover arbitrary population characteristics which vary with time, however, presents challenges. For instance, the complexities of considering stage spatially are illustrated in ongoing research (see Roper and Caswell, 2023). Until now, the demography of multi-state kinship has only been explored in the context of time-invariant population projections and rather specific descriptions of stage.

An alternative and mathematically elegant way to construct kinship networks draws from the methods of Coste et al. (2021). The authors, by defining Ego (rather than Focal) and kin through a common ancestor, utilise genealogical Markov chains (Demetrius, 1974) to count possible generational survival and reproductive events which connect the relatives. Their methods depend on a one-sex time-invariant population structured by "class". Here, the term class is intended to encompass any conceivable discrete population structure (Coste et al., 2021). Although a time-invariant assumption allows one to consider how Focal's kingship changes by age of Focal if demographic conditions are maintained indefinitely, in reality demographic conditions change with age and time. As such, so will Focal's kinship. A time-variant demography means that Focal's kinship structure will be increasingly altered the more distant kin of Focal one considers, and the more volatile changes are in demographic conditions. Moreover, in some applications, progression through classes, loosely defined, may vary in complex ways by both age and time. In this respect the appeal of the genealogical Markov chain becomes clear: the method applies under any multi-state matrix projection model.

---

* Corresponding author.
E-mail address: J.Butterick@soton.ac.uk (J.W.B. Butterick).

https://doi.org/10.1016/j.tpb.2025.02.002
Received 21 June 2024

The contribution of this research to the literature is to make explicit the extension of the work of Coste et al. (2021) to the case of time-varying demographies. We illustrate the far-reaching potential of such methods through considering complex class-structured populations whereby classes are comprised of age and stage, i.e., a multi-state model. The framework presented here (i) encompasses any stage which (in addition to age) structures a population, (ii) operates within time-variant contexts, and (iii) also recovers the case of a time-invariant demography. The innovation here is to construct a time-variant genealogical Markov chain. Then following the original synthesis of Coste et al. (2021) we project individuals backwards and forwards in time; move through family lineages; and calculate cross-generational expected age×stage distributions of kin. Through concise formulae, we provide a means to analyse the ways in which arbitrary population structures shape kinship bonds. As an example of the scope of the presented framework, we consider stages defined through spatial locations, exemplified by clusters of local authority districts (LADs) in England and Wales, and sourced from the Office for National Statistics (ONS). By application, we present novel results describing time-dependent age×geography structured kinship, and contrast these innovations to the static case (e.g., Roper and Caswell, 2023).

The structure of the rest of this article is as follows: the remaining Introduction covers terminology adopted thereafter and outlines existing theory on multi-state kinship. Section 2 sets out the proposed model of this research, beginning with a descriptive summary of our approach. In Sections 2.1 and 2.2 we introduce the mathematical theory guiding our framework; in Sections 2.3 and 2.4 we clarify how we calculate Focal's kinship network (we leave some mathematical calculations to Appendix A). An example of our model's practical use is provided in Section 3. We conclude by summarising how this research to contributes towards mathematical modelling of kinship in the Discussion (Section 4).

1.1. General notation

Let $M_{n,m}(\mathbb{R})$ denote the set of $n\times m$ matrices over the real numbers. Vectors are shown boldface and lower-case, e.g., $\mathbf{x} = (x_1, x_2, \ldots, x_n)^\dagger$ where † represents the transpose. The unit vector with a one in the ith position is written $\mathbf{e}_i$. Matrices are denoted boldface and upper-case, e.g., for a matrix with n rows and m columns, write $\mathbf{A} = \left(a_{ij}\right) \in M_{n,m}$. Block diagonal matrices, formed as a direct sums, are denoted $\mathbb{A}$. The Hadamard (element-by-element) product is denoted by $\circ$; the Kronecker product by $\otimes$; the vec-operator by vec(.); and diag(.) is interchangeably used to extract the diagonal entries of a matrix in vector form or to convert a vector into a diagonal matrix. The l_1 norm (on $\mathbb{R}^n$) is represented by $\|\mathbf{x}\|_1 = \sum_i^n |x_i|$; its extension to matrices (on $\mathbb{R}^{n\times m}$) by $\|\mathbf{A}\| = \sum_{i,j=1}^n |a_{ij}|$ and the operator norm it induces by

$$\|\!|\mathbf{A}|\!\|_1 = \sup_{\|\mathbf{x}\|_1=1} \|\mathbf{A}\mathbf{x}\|_1 = \max_{1\le j\le n} \sum_{i=1}^{n} |a_{ij}|.$$

A matrix $\mathbf{A} \in M_{n,n}$ has a spectral radius denoted $\rho(\mathbf{A})$ and spectrum $\{\lambda_i(\mathbf{A})\}$, $i = 1, \ldots, n$ (with the convention $\lambda_1 \geq \cdots \geq \lambda_n$). Lastly, we define for any arbitrary sequence of matrices $\mathcal{A} = \{\mathbf{A}_i\}_{i=a}^{b}$, the ordered product

$$\Gamma^{\mathcal{A}}(a,b) := \prod_{i=a}^{b} \mathbf{A}_i = \mathbf{A}_b \mathbf{A}_{b-1} \cdots \mathbf{A}_a,$$

$$\text{where } \Gamma^{\mathcal{A}}(a,b) = \mathbf{A}_a, \mathbf{I} \text{ respectively if } a = b, a > b.$$

1.2. The existing age×stage kin method

As our research focuses on kin of Focal defined through age and stage, here we introduce the existing multi-state model of kin. Caswell (2020) considers a population structure defined through stages $i = 1, \ldots, s$ and ages $j = 1, \ldots, n$. As such, the matrix

$$\mathbf{K} = \begin{pmatrix} k_{11} & k_{12} & \ldots & k_{1n} \\ k_{21} & k_{22} & \ldots & k_{2n} \\ \vdots & \vdots & \ddots & \vdots \\ k_{s1} & k_{s2} & \ldots & k_{sn} \end{pmatrix} \in M_{s,n} \tag{1}$$

has scalar entries k_{ij} which give the expected number of kin in stage i of age j. One proceeds to project a block-structured kinship vector defined through $\tilde{\mathbf{k}} = \text{vec}(\mathbf{K})$, by a commutation constructed time-invariant projection matrix (Magnus and Neudecker, 2019). For each age-class $j \in \{1, 2, \ldots, n\}$, one defines stage transfer matrices $\mathbf{T}_j = \left(t_{kl}^{(j)}\right) \in M_{s,s}$ with entries capturing transitions of individuals from stage l to k; and fertility matrices $\mathbf{F}_j = \left(f_{kl}^{(j)}\right) \in M_{s,s}$ with entries specifying the production of stage k individuals by stage l individuals. For each stage $i \in \{1, 2, \ldots, s\}$, one defines age-specific mortality matrices $\mathbf{U}_i = \left(u_{kl}^{(i)}\right) \in M_{n,n}$ specifying survival probabilities upwards in age-classes (i.e., from age l to k); and recombination matrices $\mathbf{H}_i = \left(h_{kl}^{(i)}\right) \in M_{n,n}$ which, independently for each stage, characterise the age-classes k of newborns from mothers of age-class l. As all newborns begin life in the first age-class, each $\mathbf{H}_i$ has a top-row of ones and all other entries zero.

By taking direct sums of the above matrices (e.g., $\mathbb{U} = \mathbf{U}_i \oplus \cdots \oplus \mathbf{U}_s$), a block-structured projection matrix $\tilde{\mathbf{A}} = \tilde{\mathbf{U}} + \tilde{\mathbf{F}}$ is generated through application of the commutation matrix $\boldsymbol{\Psi}_{q,r}$ (i.e., $\boldsymbol{\Psi}_{q,r}\text{vec}\mathbf{A} = \text{vec}\mathbf{A}^\dagger$ for $\mathbf{A} \in M_{q,r}$) (Magnus and Neudecker, 2019):

$$\tilde{\mathbf{U}} = \boldsymbol{\Psi}_{s,n}^{\dagger} \mathbb{U} \boldsymbol{\Psi}_{s,n} \mathbb{T} \quad \text{and} \quad \tilde{\mathbf{F}} = \boldsymbol{\Psi}_{s,n}^{\dagger} \mathbb{H} \boldsymbol{\Psi}_{s,n} \mathbb{F} \quad (\text{both } \in M_{sn,sn}). \tag{2}$$

The actions of the linear transformations in Eq. (2) are detailed in Caswell et al. (2018) and we refer the reader there for further details. As detailed later, our method to calculate multi-state kinship applies the same projection matrices above, however extended to time-variant situations.

Caswell (2020) derives the relation $\tilde{\mathbf{k}}(x+1) = \tilde{\mathbf{U}}\tilde{\mathbf{k}}(x) + \tilde{\boldsymbol{\beta}}(x)$ to obtain a distribution for Focal's kin when Focal is of age $x+1$. The term $\tilde{\boldsymbol{\beta}}(x)$, referred to as a "subsidy" vector, takes on values of zero in cases by which Focal cannot gain kin during its life (e.g., mothers), or $\tilde{\boldsymbol{\beta}}(x) = \tilde{\mathbf{F}}\tilde{\mathbf{k}}^*(x)$ where $\tilde{\mathbf{k}}^*(x)$ represents some producer kin within Focal's network (e.g., if $\tilde{\mathbf{k}}(x)$ is younger sister then $\tilde{\mathbf{k}}^*(x)$ is mother). A complete description of the model is given in Caswell (2019b).

The above-described method is appealing due to its simplicity and computational efficiency. However, the recursive nature of the formulation requires well-defined initial condition (i.e., at Focal's birth) for each kin-type, $\tilde{\mathbf{k}}(0)$, obtained through the so-called age×stage distribution of mothers in the population ($\tilde{\boldsymbol{\pi}}$ of Eq. (14) in Caswell, 2020). The parity-specific method to calculate the distribution of mothers proposed by Caswell (2020) exploits particular features pertaining to parity as a stage. Newborns always start in the first stage (parity zero), and then monotonically progress up stages during their lives. Importantly, $\tilde{\boldsymbol{\pi}}$ is derived under a limiting case: mothers only produce newborns in the first stage class. This restricts the model being applied to more complex stage based dynamics. One needs either to impose additional assumptions to the established model (e.g., Roper and Caswell, 2023), or an alternative model. In the next section we explain how a semi-Markov model ensures the distributions of mothers is valid in any age×stage structured population – thereby circumventing the above issues – and extend the framework to time-variant situations.

2. A time-dependent Markov model

Here we advance the theoretical methods proposed by Coste et al., 2021 to calculate time-variant multi-state kinship. The benefits of this approach are that under an appropriate projection matrix (age, stage, or jointly structured), the distributions of mothers (or any further distant ancestor) are naturally derived through Markov theory. Following the approach of Pullum (1982), we let q be the minimum genealogical

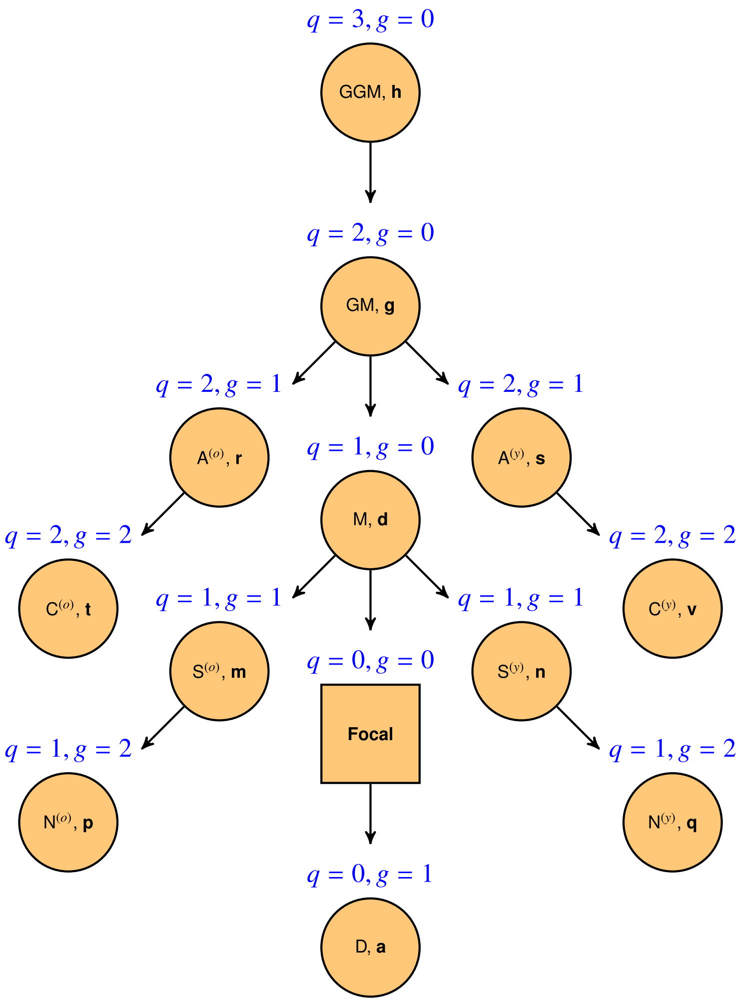

Fig. 1. Focal's family tree. q defines the number of generations we ascend Focal's family tree. g defines the number of generations we travel down Focal's family tree, starting from q. Left shoots define older lineages of Focal's family tree (superscripted "o"); right shoots define younger lineages (superscripted "y"). We use abbreviations (acronyms) for relations. For comparison to Fig. 1. Caswell (2019b) boldface letters correspond to notation therein.

distance between Focal and some common ancestor relating it to its kin. We let g be the distance from the kin and this common ancestor (e.g., Focal's sisters are defined $g = q = 1$; and daughters $g = 1, q = 0$). For a graphical illustration of the g, q relations see Fig. 1.

Our approach to calculate Focal's kin is (i): to travel backwards in time and locate Focal's qth ancestor; and (ii): to travel forwards in time and count through g generations of reproduction (and subsequent survival) emanating from Focal's qth ancestor. The next sections clarify how this is accomplished.

2.1. Genealogical Markov chains

To travel q generations up Focal's ancestry we draw from the theory of genealogical Markov chains, first introduced by Demetrius (1974, 1975) and later advanced by Tuljapurkar (1993). In those papers (and see also Coste et al., 2021), transition matrices of time-homogeneous Markov chains were applied to probabilistically infer ancestries in populations. Here, we first recapitulate how these techniques apply to kinship, and then propose an in-homogeneous Markov chain associated with a time-variant demography. We detail how to construct the Markov chain by decomposing the population structure which also varies with time in accordance with the sequences of time-dependent projection matrices.

Eqs. (1)–(2) of Coste et al. (2021) show how to infer probabilistically an individual's ancestry in a class-structured time-invariant demography. Subject to static demographic rates, the approach equally operates within a multi-state population as long as the projection matrix $\tilde{\mathbf{A}}$ (of the form given in Eq. (2)) is irreducible. In this case, Perron–Frobenius theory (e.g., 8.4.4 Horn and Johnson, 2010) guarantees a stable population structure $\tilde{\mathbf{z}}$ and growth rate $\lambda = \rho(\tilde{\mathbf{A}})$. Under these conditions, row-proportionality of the eigenvector equation $\tilde{\mathbf{A}}\tilde{\mathbf{z}} = \lambda\tilde{\mathbf{z}}$ allows one to deduce the probability that an individual currently defined through age×stage k at time $t+1$ was defined by age×stage l at time t, either in the form of itself one time-step prior or an ancestor:

$$\tilde{p}_{kl}(t) = \frac{\tilde{a}_{kl}\tilde{z}_l}{\lambda\tilde{z}_k} = \underbrace{\frac{\tilde{u}_{kl}\tilde{z}_l}{\lambda\tilde{z}_k}}_{\tilde{v}_{kl}(t)} + \underbrace{\frac{\tilde{f}_{kl}\tilde{z}_l}{\lambda\tilde{z}_k}}_{\tilde{w}_{kl}(t)}. \tag{3}$$

Through Eq. (3) we observe two types of genealogical transitions. Between-genealogy transitions are driven by fertility and recombination components of the projection matrix (i.e., elements of $\mathbf{F}_j$ and $\mathbf{H}_i$ – see Section 1.2). Such transitions are encapsulated in $\tilde{w}_{kl}(t)$: the probability that an individual of age×stage k at time $t+1$ was produced by an ancestor in age×stage l at time t. Within-genealogy transitions are driven by survival and stage-transition components of the projection matrix (elements of $\mathbf{U}_i$ and $\mathbf{T}_j$ – see Section 1.2), as captured by $\tilde{v}_{kl}(t)$: the probability that an individual of age×stage k at time $t+1$ was extant (alive) at time t, and of age×stage l.

In most applications, demographic rates change with time. Using the stable population structure to calculate $\tilde{p}_{kl}(t)$ as in Eq. (3) is no longer

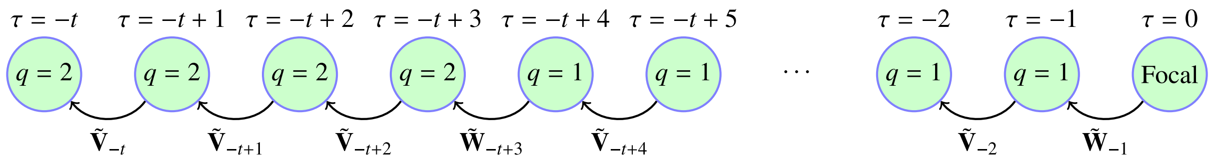

Fig. 2. Projecting up Focal's genealogy. Right to left: at time $\tau = 0$, Focal is born with distribution $\tilde{\boldsymbol{\phi}}_0$. Operating on Focal's initial distribution by $\tilde{\mathbf{W}}_{-1}$ yields the distribution of Focal's mother at time-step prior to birth of Focal ($t_1 = -1$). Focal's mother is extant between times $\tau = -1$ and $\tau = -t+4$ in the past, at which her distribution is given by $\tilde{\mathbf{V}}_{-2} \cdots \tilde{\mathbf{V}}_{-t+4}$. At time step $\tau = -t+4$ the action of $\tilde{\mathbf{W}}_{-t+3}$ yields Focal's grandmother's distribution at time step prior to birth of Focal's mother ($t_2 = -t+3$). Subsequent application by $\tilde{\mathbf{V}}_{-t+2}\tilde{\mathbf{V}}_{-t+1}\tilde{\mathbf{V}}_{-t}$ defines Focal's grandmother's distribution – conditional on her being alive – at time $\tau = -t$.

appropriate (Caswell, 2022). This is because within a time-varying demography, the present time period's population structure will not reflect the stable structure derived from that period's demographic rates. Instead, it will be affected by inertia from the previous time period's population structure. The population structure varies with time. To model such temporal effects, we suppose that Focal is born at time period $\tau = 0$. Consider the sequences of age×stage-structured matrices capturing age-advancement and stage transitions:

$$\mathcal{U} = \tilde{\mathbf{U}}_{-m}, \tilde{\mathbf{U}}_{-m+1}, \dots \tilde{\mathbf{U}}_0, \dots, \tilde{\mathbf{U}}_{n-1}, \tilde{\mathbf{U}}_n, \quad \text{where } \tilde{\mathbf{U}}_i \in M_{sn,sn},$$

and reproduction along with age×stage allocation of newborns:

$$\mathcal{F} = \underbrace{\tilde{\mathbf{F}}_{-m}, \tilde{\mathbf{F}}_{-m+1}, \dots, \tilde{\mathbf{F}}_{-1}}_{\text{prior to birth of Focal}}, \tilde{\mathbf{F}}_0, \underbrace{\tilde{\mathbf{F}}_1, \dots, \tilde{\mathbf{F}}_{n-1}, \tilde{\mathbf{F}}_n}_{\text{after birth of Focal}}, \quad \text{where } \tilde{\mathbf{F}}_i \in M_{sn,sn},$$

comprising projection matrices $\tilde{\mathbf{U}}_t + \tilde{\mathbf{F}}_t = \tilde{\mathbf{A}}_t = \left(\tilde{a}_{ij}(t)\right) \in M_{sn,sn}$ where $\mathcal{A} := \{\tilde{\mathbf{A}}_i\}_{i=-m}^{n}$. Given our earliest available set of time-varying demographic rates, say at $\tau = -m$, we impose a time boundary condition. That is, we suppose that the rates have been in effect for a sufficiently long enough time to result in a stable population structure prior to the boundary. We assume that $\tilde{\mathbf{A}}_{-m}$ is irreducible, apply $\tilde{\mathbf{A}}_{-m}\tilde{\mathbf{z}}_{-m} = \lambda(-m)\tilde{\mathbf{z}}_{-m}$ with $\|\tilde{\mathbf{z}}_{-m}\|_1 = 1$, and set $\tilde{\mathbf{z}}_{-m}$ as the boundary (or initial) population structure. For each time $t > -m$ we then project a transient population structure $\tilde{\mathbf{z}}_t$, appropriately normalised to sum to one. The transient population structure is recursively derived through

$$\tilde{\mathbf{z}}_{t+1} = \frac{\tilde{\mathbf{A}}_t\tilde{\mathbf{z}}_t}{\|\tilde{\mathbf{A}}_t\tilde{\mathbf{z}}_t\|_1} \text{ with } \tilde{\mathbf{z}}_t = \frac{\Gamma^{\mathcal{A}}(-m+1, t-1)\tilde{\mathbf{z}}_{-m}}{\|\tilde{\mathbf{A}}_{t-1}\tilde{\mathbf{z}}_{t-1}\|_1 \cdots \|\tilde{\mathbf{A}}_{-m+1}\tilde{\mathbf{z}}_{-m+1}\|_1}. \tag{4}$$

Eq. (4) describes how the relative proportions of individuals in different stages and ages change with time. Noting that the transient growth rate is $\lambda(t) = \|\tilde{\mathbf{A}}_t\tilde{\mathbf{z}}_t\|_1$, we can extend Eq. (3) to cover time-variant demographics: the probability an individual in age×stage k at $t+1$ came from age×stage l at time t is given by

$$\tilde{p}_{kl}(t) = \frac{\tilde{a}_{kl}(t)\tilde{z}_l(t)}{\lambda(t)\tilde{z}_k(t+1)} \text{ for } t > -m, \quad \tilde{p}_{kl}(t) = \frac{\tilde{a}_{kl}(-m)\tilde{z}_l(-m)}{\lambda(-m)\tilde{z}_k(-m)} \text{ for } t \leq -m \tag{5}$$

where we again decompose $\tilde{a}_{kl}(t) = \tilde{u}_{kl}(t) + \tilde{f}_{kl}(t)$ so that for $t > -m$

$$\tilde{v}_{kl}(t) = \frac{\tilde{u}_{kl}(t)\tilde{z}_l(t)}{\lambda(t)\tilde{z}_k(t+1)} \text{ and } \tilde{w}_{kl}(t) = \frac{\tilde{f}_{kl}(t)\tilde{z}_l(t)}{\lambda(t)\tilde{z}_k(t+1)}.$$

Note that Eq. (5) is well-defined because $\tilde{\mathbf{z}}_t$ remains strictly positive. That is, irreducibility of each $\tilde{\mathbf{A}}_t$ – through the fact that the matrix contains no zero row or column – ensure that $\tilde{\mathbf{z}}_{t+1} > 0$.

To summarise our dynamic modelling of the population structure, for the first available set of demographic rates we apply Eq. (3) (cf. the right hand side of Eq. (5)), and then apply Eq. (5) thereafter. Then, for each projection matrix $\tilde{\mathbf{A}}_t$ we form an associated backwards time in-homogeneous Markov chain with transition matrix $\tilde{\mathbf{P}}_t = \left(\tilde{p}_{kl}(t)\right) \in M_{sn,sn}$, decomposed such that $\tilde{\mathbf{P}}_t = \tilde{\mathbf{V}}_t + \tilde{\mathbf{W}}_t$. Recall the entries of $\tilde{\mathbf{V}}_t = \left(\tilde{v}_{kl}(t)\right)$ provide probabilities that individuals in age×stage k at time $t+1$ were extant (alive) at time t, and in age×stage l; the entries of $\tilde{\mathbf{W}}_t = \left(\tilde{w}_{kl}(t)\right)$ yield probabilities that individuals in age×stage k at time $t+1$ were produced by an ancestor in age×stage l at t. We denote the time-ordered sequences of transition matrices for the genealogical Markov chain

$$\mathcal{V} = \tilde{\mathbf{V}}_{-m}, \tilde{\mathbf{V}}_{-m+1}, \dots \tilde{\mathbf{V}}_{-1}, \text{ and}$$

$$\mathcal{W} = \tilde{\mathbf{W}}_{-m}, \tilde{\mathbf{W}}_{-m+1}, \dots, \tilde{\mathbf{W}}_{-1}, \ (\text{all } \in M_{sn,sn}).$$

As a simple example of the time-inhomogeneous Markov chain, suppose an individual is of exact age n^* and stage s^* at time $\tau = 0$. The individual can be represented by an element of a matrix similar to Eq. (1)). In vectorised form the individual is represented by the $s*$ –th entry of the $(n^* - 1)$-th block of a unit vector of length sn. That is, $\tilde{\mathbf{e}}_L$ where $L = s(n^* - 1) + s^*$. The operation $\tilde{\mathbf{e}}_L^\dagger \tilde{\mathbf{P}}_{-1}$ provides a probability distribution for the genealogical age×stage of that individual at time $\tau = -1$ (either as a itself one year in the past or its mother). For further details on genealogical Markov chains see Bienvenu et al. (2017).

Decomposing $\tilde{\mathbf{P}}_t$ into genealogical survival and reproductive transitions is central to the mathematical framework developed by Coste et al., 2021, and is no less important in the time varying case; it allows one travel between and within generations of Focal's ancestry. For instance, the matrix $\Gamma^{\mathcal{V}}(-t+1, -1)\tilde{\mathbf{W}}_{-t}$ has (i, j) entry equal to the probability that an individual in age×stage i at time $\tau = 0$ was extant between times $\tau = -t+1$ and $\tau = 0$, but was born to an ancestor in age×stage j during the open interval between $\tau = -t$ and $\tau = -t+1$. All we require to project Focal's kin backwards and forwards is some well defined distribution for Focal at birth:

$$\tilde{\boldsymbol{\phi}}_0 = \left(\phi_1(0), \phi_2(0), \ \dots \ \phi_s(0) \mid 0 \ \dots 0 \mid \ \dots \ \mid 0 \ \dots \ 0\right)^\dagger \tag{6}$$

where obviously $\phi_1(0) + \cdots + \phi_s(0) = 1$ (since Focal must be in one stage or some mixture of stages). Note that, as representative of many relevant demographic characteristics, e.g., parity (Caswell, 2020), educational attainment (Song and Mare, 2019) or geography (Raymer et al., 2019), if Focal is born into one unique stage $s^* \in \{1, \dots, s\}$ the entries of Eq. (6) would reduce to $\phi_i(0) = \delta_{i-s^*}$ where δ_x is the Kronecker delta function (i.e., $\delta_0 = 1$ and $\delta_k = 0 \ \forall k \neq 0$). Uniqueness of Focal's stage at birth is not a pre-requisite of our model but is appropriate in an application we present (see Section 3).

2.2. Counting kin

To obtain the distribution of g, q kin at any age x of Focal, we adopt similar methods proposed by Coste et al. (2021). In particular, we apply in parallel two independent processes. In one process we travel up Focal's genealogy (backwards in time), applying time-dependent genealogical Markov chains and seeking the age×stage distribution of Focal's qth ancestor. At each time τ prior to Focal's birth, q generations of Focal's ancestry are defined through that many time-ordered genealogical reproductive transitions. Let t_i define the start of the interval of the genealogical transition from Focal's $(i-1)^{th}$ ancestor to Focal's ith ancestor. We know that the first genealogical reproductive transition is from Focal to Focal's mother, defined at $t_1 = -1$. An illustrative example of a genealogical sequence from Focal to Focal's grandmother ($q = 2$) is given in Fig. 2.

In the other process, we travel down Focal's genealogy (forwards in time) using projection matrices in order to derive distributions Focal's qth ancestor's descendants. From each time τ whereby we have obtained Focal's qth ancestor's conditional distribution, we probabilistically count all possible ways that g generations of descendants of Focal's qth ancestor can be spanned up to age x of Focal. Define s_i as the time at which the ith-generation descendent of Focal's qth ancestor

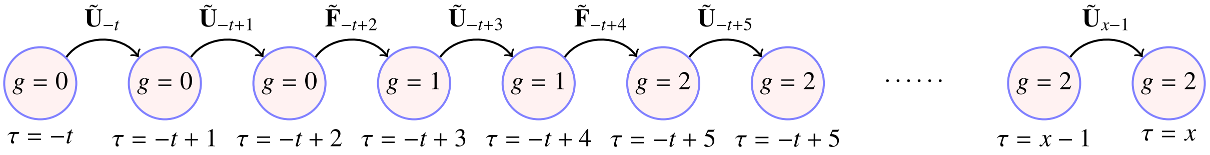

Fig. 3. Projecting down Focal's genealogy. Left to right: suppose at time $\tau = -t$ we know the distribution of some direct ancestor of Focal ($g = 0$). Focal's ancestor does not produce offspring until time $\tau = -t+2$ when the action of $\tilde{\mathbf{F}}_{-t+2}$ defines $g = 1$ (so $s_1 = -t+2$). The $g = 1$ kin of Focal survives to time step $\tau = -t+3$ and reproduces at $\tau = -t+4$ producing the $g = 2$ kin (so $s_2 = -t+4$). For illustrative purposes, we assume that this kin survives (at least) until time $\tau = x$.

is born. An illustrative example of using projection matrices to span $g = 2$-generations of descendants is shown in Fig. 3.

As in Coste et al. (2021), the above-mentioned processes, independently applied, allow us to calculate distributions of any g, q kin of Focal. We note that direct ancestors and descendants of Focal reduce to special instances. Ancestors, defined through $g = 0$ are detailed in Section 2.3, while descendants, defined through $q = 0$ require special consideration depending on whether we subject Focal to mortality risk (see Section 2.4). While we consider kin of Focal which are neither direct ancestors nor descendants, we consider two diametrically opposite cases: kin may descend from younger or older siblings of Focal's $(q-1)^{th}$ ancestor. These cases, respectively, are explained in Appendix A.1. We observe that our model reproduces the case presented by Coste et al. (2021) in which time-invariant projection matrices are used. The time ordered products of demographic matrices considered here reduce to matrix powers, i.e., $\Gamma^{\mathcal{V}}(1, n) \to \tilde{\mathbf{U}}^n$.

2.3. *Kin which descend from younger siblings of Focal's $(q-1)^{th}$ ancestor, and Focal's ancestors*

Younger lineages of Focal's family tree are graphically illustrated by the right offshoots of Fig. 1. By definition, Focal's kin must be produced by its qth ancestor at some time "after" Focal's $(q-1)^{th}$ ancestor is produced; see Fig. 4.

2.3.1. *Up Focal's genealogy to its qth ancestor*

Here we seek to project backwards time steps prior to Focal being born and obtain the age×stage distribution for Focal's qth ancestor, at time step prior to birth of Focal's $(q-1)^{th}$ ancestor. We know that the first genealogical reproductive transition is from Focal to Focal's mother. As such, recalling the definition of t_i we fix $t_1 = -1$. We fix at some time $\tau = -t$ in the past, the final genealogical reproductive transition $\tilde{\mathbf{W}}_{t_q}$ so $t_q = -t$. To obtain a t−conditional distribution for Focal's qth ancestor one time step before birth of Focal's $(q-1)^{th}$ ancestor, we count over possible sequences of the $q-2$ intermediate genealogical reproductive transitions $\{\tilde{\mathbf{W}}_{t_i}\}_{i=2}^{q-1}$, interspersed by genealogical survival transitions.

Formally, we define the vector $\mathbf{t} = (t_1, t_2, t_3, \dots, t_q)^\dagger \in \mathbb{Z}^q$ with $t_1 = -1$ and $t_q = -t$. We define the ordered matrix product

$$\begin{aligned}\Lambda(q) := {} & \tilde{\mathbf{W}}_{t_1}\Gamma^{\mathcal{V}}(t_2+1, t_1-1)\tilde{\mathbf{W}}_{t_2}\Gamma^{\mathcal{V}}(t_3+1, t_2-1)\tilde{\mathbf{W}}_{t_3}\cdots \\ & \tilde{\mathbf{W}}_{t_{q-1}}\Gamma^{\mathcal{V}}(t_q+1, t_{q-1}-1)\tilde{\mathbf{W}}_{t_q}\end{aligned}$$

with the convention that $\Lambda(1) = \tilde{\mathbf{W}}_{-1}$, and the set

$$\mathcal{S}_t^q := \{\mathbf{t} \in \mathbb{Z}^q : t_1 > \cdots > t_q\} \text{ where } \mathcal{S}_t^0 = \emptyset\ \forall t,\ \ \mathcal{S}_t^1 = \begin{cases} \emptyset & t > 0 \\ \{0\} & t = 0 \end{cases}.$$

Next we construct the function

$$\boldsymbol{\mathcal{K}}^{\mathrm{b}}(q, t) := \tilde{\boldsymbol{\phi}}_0^\dagger \sum_{\mathbf{t}\in\mathcal{S}_t^q} \Lambda(q). \tag{7}$$

Eq. (7) gives Focal's qth ancestor's distribution one time-step before giving birth to Focal's $(q-1)^{th}$ ancestor, conditioned on the final genealogical reproductive transition occurring precisely at $\tau = -t$. Summing over all possible times in the past $t \geq 0$ provides the full distribution for Focal's qth ancestor one time-step before giving birth to Focal's $(q-1)^{th}$ ancestor. An example is presented in Box 1.

Box 1 Focal's qth Ancestor's Distribution at Birth Of Focal's $(q-1)^{th}$ Ancestor

Consider an example of a great-grandmother, $q = 3$:

$$\begin{aligned}&\sum_{t\geq 0}\left(\boldsymbol{\mathcal{K}}^{\mathrm{b}}(3, t)\right)^\dagger = \sum_{t>0}\tilde{\boldsymbol{\phi}}_0^\dagger \sum_{\mathbf{t}\in\mathcal{S}_t^3}(\Lambda(3))^\dagger \\ &= \sum_{t\geq 0}\sum_{-1>t_2>t_3=-t\in\mathbb{R}}\left(\tilde{\boldsymbol{\phi}}_0^\dagger\tilde{\mathbf{W}}_{-1}\Gamma^{\mathcal{V}}(t_2+1, -2)\tilde{\mathbf{W}}_{t_2}\Gamma^{\mathcal{V}}(-t+1, t_2-1)\tilde{\mathbf{W}}_{-t}\right)^\dagger \\ &= \sum_{t\geq 0}\sum_{t_2=-t+1}^{-2}\left(\tilde{\boldsymbol{\phi}}_0^\dagger\tilde{\mathbf{W}}_{-1}\Gamma^{\mathcal{V}}(t_2+1, -2)\tilde{\mathbf{W}}_{t_2}\Gamma^{\mathcal{V}}(-t+1, t_2-1)\tilde{\mathbf{W}}_{-t}\right)^\dagger.\end{aligned} \tag{8}$$

Eq. (8) yields the age×stage distribution for Focal's great-grandmother when producing Focal's grandmother. For fixed t, t_2 the summand term provides a conditional age×stage distribution:

- $\tilde{\boldsymbol{\phi}}_0^\dagger\tilde{\mathbf{W}}_{-1}\Gamma^{\mathcal{V}}(t_2+1, -2)$ gives the distribution for Focal's mother, given that she was extant over a period from $\tau = -1$ to $\tau = t_2 + 1$.
- Right multiplication by $\tilde{\mathbf{W}}_{t_2}$ provides Focal's grandmother's distribution when producing Focal's mother, conditional on this event occurring between $\tau = t_2$ and $\tau = t_2 + 1$.
- Right multiplication by $\Gamma^{\mathcal{V}}(-t+1, t_2-1)$ provides Focal's grandmother's distribution at $\tau = -t + 1$, given that grandmother was extant between $\tau = t_2 - 1$ and $\tau = -t+1$.
- Right multiplication by $\tilde{\mathbf{W}}_{-t}$ yields Focal's great-grandmother's distribution at time $\tau = -t$, conditional on Focal's great-grandmother producing Focal's grandmother between times $\tau = -t$ and $\tau = -t + 1$.

For fixed t, the t_2−summation produces great-grandmother's distribution (at birth of Focal's grandmother), conditional on the probability that Focal's grandmother was procured between $\tau = -t$ and $\tau = -t + 1$. Summation over all t produces a full distribution for Focal's great-grandmother at birth of Focal's grandmother.

2.3.2. *Down Focal's genealogy g generations from its qth ancestor*

For each t−conditional distribution of Focal's qth ancestor at timestep prior to birth of Focal's $(q-1)^{th}$ ancestor, we concurrently project forwards in time, counting Focal's qth ancestor's g−generation descendants. Focal's $(q-1)^{th}$ ancestor is born between times $\tau = -t$ and $\tau = -t + 1$ and the distribution for Focal's qth ancestor is defined at $\tau = -t$. To ensure Focal's kin descend through younger siblings of Focal's $(q-1)^{th}$ ancestor, we must count reproductive events which occur strictly after the time $\tau = -t + 1$. As such, the expected number of kin when Focal is aged x is found by counting permutations of reproductions over a time period $t + x$ (i.e., from $\tau = -t + 1$ up to $\tau = x - 1$).

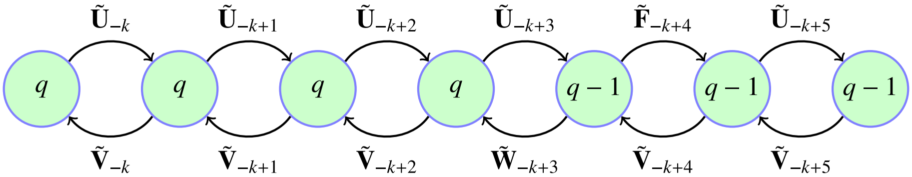

Fig. 4. Younger lineages: kin which descend from younger siblings of Focal's $(q-1)^{th}$ **ancestor**. A specific sequence of demographic events. Right to left: the genealogical Markov chains define production of Focal's $(q-1)^{th}$ ancestor by Focal's qth ancestor through the action $\tilde{\mathbf{W}}_{-k+3}$. Left to right; projection matrices define the descendants of Focal's qth ancestor. The action of $\tilde{\mathbf{F}}_{-k+4}$ produces an offspring of Focal's qth ancestor, born after Focal's $(q-1)^{th}$ ancestor, i.e., a younger sibling of Focal's $(q-1)^{th}$ ancestor.

Recalling the definition of s_i, we define $\mathbf{s} = (s_0, s_1, s_2, \dots, s_g)^\dagger \in \mathbb{Z}^{g+1}$, where $-t = s_0$ and $s_0 \leq s_1 < s_2 < \dots < s_g < x$, and the ordered product

$$\Delta(g) := \Gamma^{\mathcal{U}}(s_g+1, x-1)\tilde{\mathbf{F}}_{s_g}\Gamma^{\mathcal{U}}(s_{g-1}+1, s_g-1)\tilde{\mathbf{F}}_{s_{g-1}} \cdots \tilde{\mathbf{F}}_{s_1}\Gamma^{\mathcal{U}}(s_0, s_1-1)$$

with the convention that $\Delta(0) = \Gamma^{\mathcal{U}}(-t, x-1)$, whereas $\Delta(1) = \Gamma^{\mathcal{U}}(s_1+1, x-1)\tilde{\mathbf{F}}_{s_1}\Gamma^{\mathcal{U}}(-t, s_1-1)$. The product $\Delta(g)$ defines one realisation of g reproductive events over the timescale $\tau = -t, \dots, 0, \dots, x$. We define the set

$$\mathcal{Q}^g_{t,x} = \{\mathbf{s} \in \mathbb{Z}^{g+1} : -t = s_0 \leq s_1 < s_2 < \dots < s_g < x\}, \;\; \mathcal{Q}^0_{t,x} = -t \;\; \forall t, x$$

and function

$$\boldsymbol{\mathcal{K}}^{\mathrm{f}}(g,t,x) := \sum_{\mathbf{s} \in \mathcal{Q}^g_{t,x}} \Delta(g). \tag{9}$$

Eq. (9) counts all permutations of g (time-ordered) reproductions from $\tau = -t$ to $\tau = x$. Summing over potential timescales $t \geq 0$ specifies how far backwards in time we travel. Notice that if $g = 0$, by definition of the set $\mathcal{Q}^g_{t,x}$ one observes that Eq. (9) reduces to a sum over one element; $s_0 = -t$. In this case we recover $\Gamma^{\mathcal{U}}(s_0, x) = \tilde{\mathbf{U}}_{x-1} \cdots \tilde{\mathbf{U}}_{-t}$, meaning that summing over t simply yields survival from each $\tau = -t$ up to $\tau = x$. For an example when $g > 0$, see Box 2.

Box 2 Counting g Generations of Descent From q

As an example, from an arbitrary time $\tau = -t$ second-generation ($g = 2$) descendants are defined by

$$\begin{aligned}\sum_{t\geq 0} \boldsymbol{\mathcal{K}}^{\mathrm{f}}(2,t,x) &= \sum_{t \geq 0} \sum_{\mathbf{s} \in \mathcal{Q}^2_{t,x}} \Delta(2) \\ &= \sum_{t\geq 0} \sum_{(s_1,s_2) \in \mathcal{Q}^2_{t,x}} \Gamma^{\mathcal{U}}(s_2+1, x-1)\tilde{\mathbf{F}}_{s_2} \\ &\quad \times \Gamma^{\mathcal{U}}(-s_1+1, s_2-1)\tilde{\mathbf{F}}_{s_1}\Gamma^{\mathcal{U}}(-t, s_1-1) \\ &\equiv \sum_{t\geq 0} \sum_{k=-t+1}^{x-2} \sum_{j=1}^{x-k} \Gamma^{\mathcal{U}}(k+j+1, x-1)\tilde{\mathbf{F}}_{k+j} \\ &\quad \times \Gamma^{\mathcal{U}}(k+1, k+j-1)\tilde{\mathbf{F}}_k \Gamma^{\mathcal{U}}(-t, k-1).\end{aligned} \tag{10}$$

Eq. (10), for each fixed time t, counts the permutations of $\mathbf{s} \in \mathcal{Q}^2_{t,x}$, i.e., the number of ways of choosing two reproductive events from a set of $t + x$ demographic events.

2.3.3. *Expected distribution for kin*

The Markov process which ascends Focal's family tree to ancestor q is independent from the matrix projections which span g generations of descendants. As such, taking the product of the t-summations of Eq. (7) and Eq. (9) collapses into a one summation over t. We therefore recover the expected distribution of Focal's kin, when Focal is aged x:

$$\mathcal{Y}(g,q,x) = \sum_{t \geq 0} \boldsymbol{\mathcal{K}}^{\mathrm{f}}(g, t-1, x)\tilde{\mathbf{U}}_{-t}\big(\boldsymbol{\mathcal{K}}^{\mathrm{b}}(q,t)\big)^\dagger. \tag{11}$$

Distributions of direct ancestors of Focal can be derived by applying to Eq. (11) with $g = 0$.

Eq. (11) provides, in column vector form, a joint age×stage distribution for Focal's g, q kin. A marginal age distribution (summing over all stages) is recovered through the operation $\big(\mathbf{I}_n \otimes \mathrm{diag}^\dagger(\mathbf{I}_s)\big)\mathcal{Y}(g,q,x)$, whereas a marginal stage distribution (summing over all ages) can be derived through $\big(\mathrm{diag}^\dagger(\mathbf{I}_n) \otimes \mathbf{I}_s\big)\mathcal{Y}(g,q,x)$. Note that if we omit time-variation from our model then we are able to recover Eq (6) from Coste et al. (2021). By application of the same logic and following the structure of the model of those authors, one can derive time-variant version of the equations for kin descending from older siblings of ancestors of Focal as well as those of siblings born in the same age class. Explicit formulae and examples are respectively given in Appendix A.1 and Appendix A.2.

2.4. *Direct descendants of Focal*

Focal's descendants' age×stage distributions depend on whether we subject Focal to the same mortality risks as the rest of the population. We would like to infer Focal's kinship structure as an age-dependent property of Focal, i.e., conditional on Focal reaching some certain age. As such, while projecting Focal we must construct a matrix $\tilde{\mathbf{X}}$ which accounts for stage transitions but ensures that Focal survives at each time-step. We derive this matrix as follows: for each stage we set column stochastic age-advancement matrices with only non-zero entries being ones on the sub-diagonal and n, n entry. The direct sum $\mathbb{X} = \mathbf{X} \oplus \mathbf{X} \oplus \cdots \oplus \mathbf{X}$ is then be subjected to the commutation procedure: $\tilde{\mathbf{X}} = \boldsymbol{\Psi}^\dagger_{nm}\mathbb{X}\boldsymbol{\Psi}_{nm}\mathbb{T}$.

Focal's direct descendants are calculated through

$$\mathcal{D}(g;x) = \boldsymbol{\mathcal{G}}^{\mathrm{f}}(g,x)\tilde{\boldsymbol{\phi}}_0 \tag{12}$$

where the definitions in Section 2.3 have been adjusted as follows:

$$\Delta^*(g) := \Gamma^{\mathcal{U}}(s_g+1, x-1)\tilde{\mathbf{F}}_{s_g}\Gamma^{\mathcal{U}}(s_{g-1}+1, s_g-1)\tilde{\mathbf{F}}_{s_{g-1}} \cdots \tilde{\mathbf{F}}_{s_1}\tilde{\mathbf{X}}^{s_1-1} \tag{13}$$

(the matrix power ensures that Focal survives with certainty over time period $s_1 - 1$) and

$$\boldsymbol{\mathcal{G}}^{\mathrm{f}}(g,x) := \sum_{\mathbf{s} \in \mathcal{Q}^g_{0,x}} \Delta^*(g). \tag{14}$$

3. Application: A multi-regional kinship model

Geography is one characteristic which defines human populations. Focal's kin can be born into any spatial location, and migrate between locations before or during Focal's life. Here we apply to a simple geographic description of stage with the aim of showcasing our model's practical use. We consider female only age-specific population sizes at the mid-year point, and use data from the Office for National Statistics (ONS) over a period 1993–2018, across 374 (as of 2021) Local Authority Districts (LADs) in ONS (2023c,b).

Population sizes by 5-year age-class and LAD over the period are official ONS mid-year estimates, sourced through the 'NOMIS' portal (NOMIS, 2023). Fertility data consists of the number of births by LAD and 5-year age-class (15–19 to 40–44) over the period (ONS, 2023c). Mortality data comprises total number of deaths by LAD and 5-year age-class (0–4 to 90–94) over the period (ONS, 2023a). Internal migration data comprises of in- and out-flow numbers between LADs by 5-year age-classes (0–4 to 90–94) (ONS, 2023b). In order to obtain and extended range of time-variant demographic rates we consider ONS

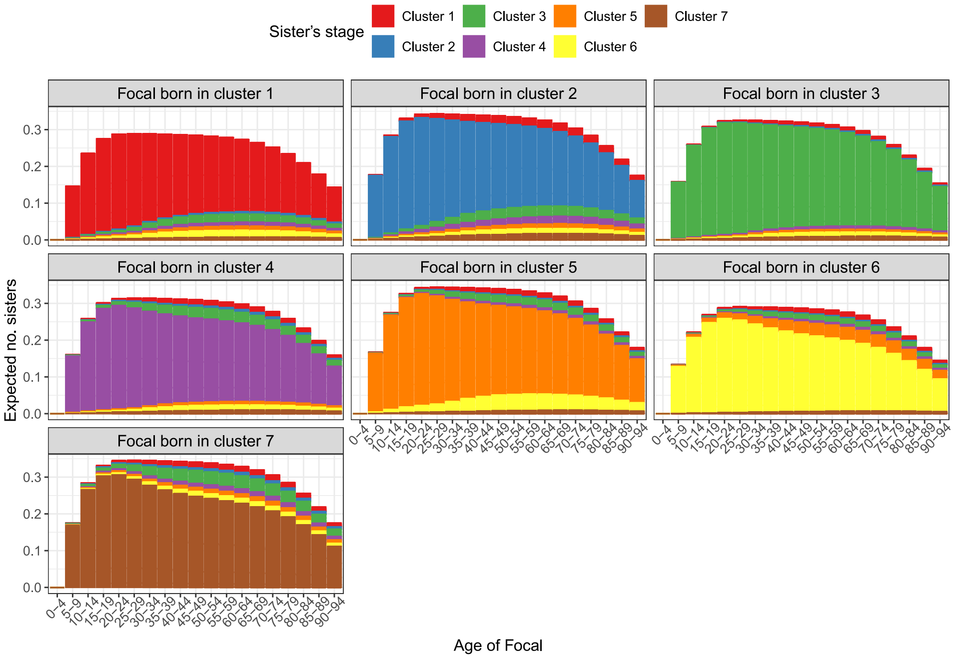

Fig. 5. $g = 1, q = 1$: Spatial distribution of Focal's younger sisters as a function of Focal's age, x.

projections for births, deaths, and population sizes, by LAD and 5-year age-class over the period 2023–2043. Projected population sizes and death counts comprise of age-classes 0–4 to 85–89 (ONS, 2023g,f). Projected number of births consist of age-classes 15–19 to 40–44 (ONS, 2023e).

We apply a $K-$means clustering algorithm based on age-specific migration out-flows to categorise LADs into one of $s = 7$ stages: $K_i, i = 1, \ldots, 7$. Grouping similar local authorities together allows us to examine the kinship structures implied by the demographic regimes currently prevailing in different types of geographic region. We use time-averaged migration counts: we do not suppose clusters are dynamic. Further details on the clustering procedure are given in Appendix B.1.

As a result of the clustering, the age-specific transfer matrices $\mathbf{T}_j$ are static, having (k, l) entries; the probability that an individual in age-class j currently in cluster l, will in 5-years have moved to cluster k. See Appendix B.2 for details on the matrix construction. The time-variant matrices $\mathbf{U}_i(t), \mathbf{F}_i(t)$ (see Section 1.2) are constructed by yearly averaging demographic rates over LADs, within each specific cluster. Details on the matrix constructions are respectively provided in Appendix B.4 and Appendix B.3.

To inform the time-invariant model, we time-average (over 1993–2018) demographic rates within each cluster. To inform the time-variant model we concatenate the data and projections, so that we have a period T spanning 1993 to 2043 by 5-year gaps. For time-periods T^* after 2043, we (i) assume age-specific mortality is constant across cluster and apply ONS national mortality projections (ONS, 2023d), and (ii) assume between cluster age-specific fertility remains the same as it is projected to be for the year 2043.

Section 3.1 presents our model results under the assumption of time-invariance. The findings are valid in the case that all of Focal's family tree experience the same set of age-specific demographic rates. As mentioned, this assumption is violated in reality when demographic rates change with time. Section 3.2 demonstrates the innovations in Focal's kinship under time-variant rates.

3.1. Application results: the time-invariant case

Here, examples of kin which descend from younger and older lineages of Focal's $(q-1)^{th}$ ancestor are presented. All illustrations within this subsection are presented as stacked bar plots: each figure depicts total accumulated kin with respective stage-specific proportions. A visualisation of how stages (clusters) are spatially spread across the UK is available upon request.

The expected age×stage distribution of Focal's younger sister as a function of Focal's age is shown in Fig. 5. Note that as we are working in discrete age-classes, the time period of Focal's birth is defined by the age-class 0–4. By definition of the mathematical simplifications we make – namely the separation of kin into descendants of younger, older, and same-age-class sisters – during this interval our Focal has no younger sisters. Between the ages of 5 and 9 Focal experiences its largest accumulation of younger sisters. Younger sisters have non-zero probabilities to be born into different clusters than the cluster Focal was born into. Nonetheless, it is unlikely that Focal's mother moves from one cluster to another within the period between Focal's birth and the birth of Focal's younger sister's birth. By the age-class 20–24, Focal has accumulated its maximum number of younger sisters. Focal has accumulated its maximum amount of older sisters at time of birth; Fig. 6. Focal is not necessarily born into the same cluster that its older sister currently resides in. However, we expect that it is unlikely for either Focal's mother to move cluster between producing Focal's older sister and producing Focal, or older sister to move cluster between her birth and birth of Focal. The expected number of older sisters monotonically decreases with age of Focal (they can only die).

In addition to viewing accumulated kin as a function of Focal's age, it is insightful to consider the expected distributions of kin given some fixed age of Focal. Fig. 7 demonstrates the age×stage distribution for Focal's older sisters when Focal is in age-class 20–24. The discontinuity along the x-axis is consonant with sisters being strictly older than Focal (classes 25–29, …). We expect a negligible amount of sisters to occupy age-classes greater than 45–49.

3.2. Application results: the time-variant case

The time-variant model allows us to compare distributions for Focal's kin from one period to another, i.e., as a function of Focal's cohort of birth. Average Focal individuals, born at different time periods, will experience differing demographic rates and consequently accumulate different amounts of various kin. To illustrate, here we project potential Focal individuals from the year 1943 (assuming static rates to

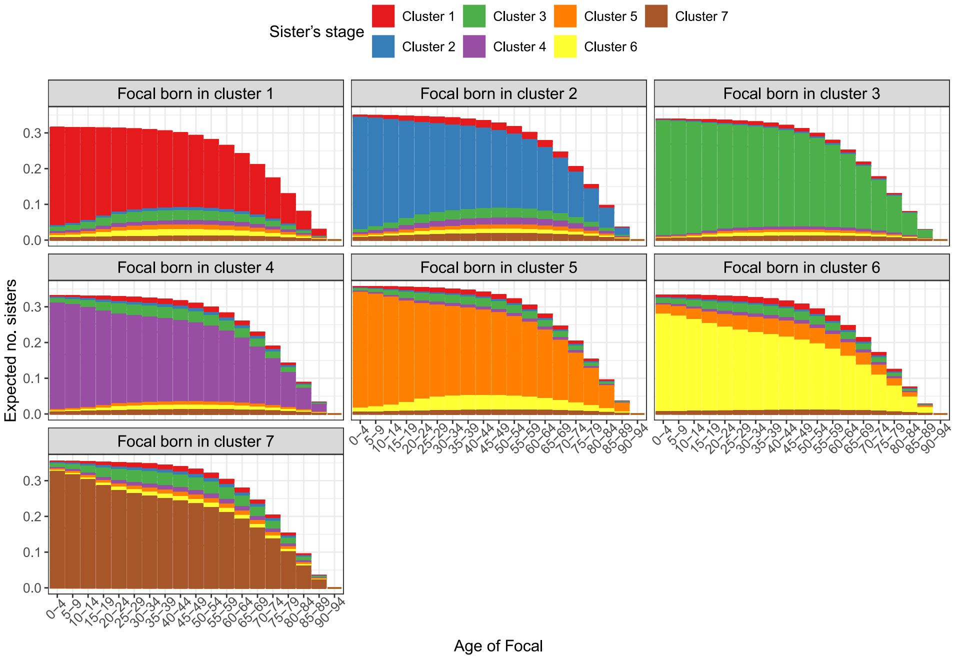

Fig. 6. $g = 1, q = 1$: Spatial distribution of Focal's older sisters as a function of Focal's age, x.

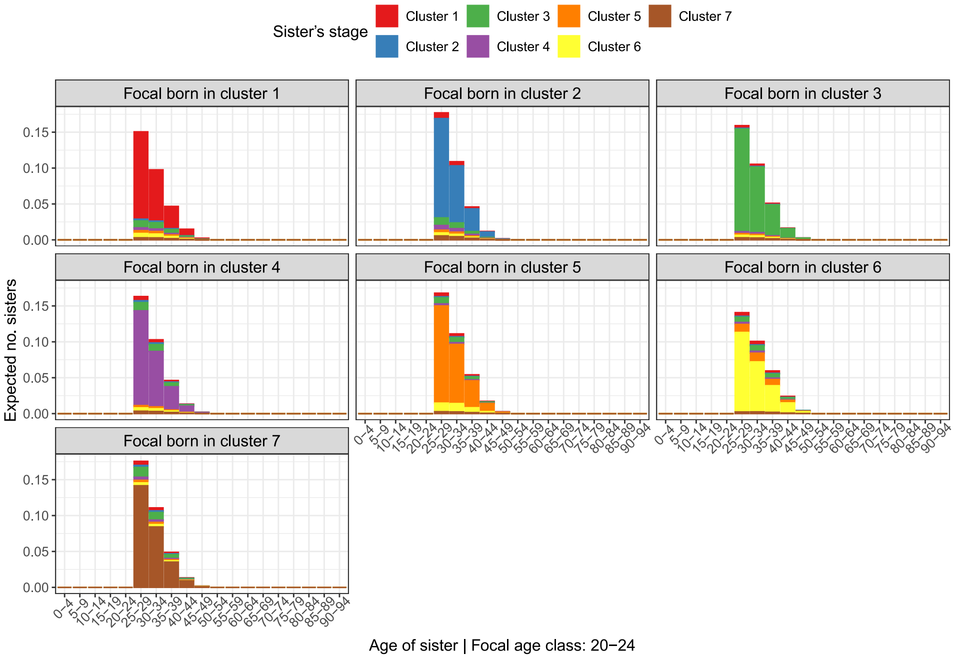

Fig. 7. $g = 1, q = 1$: Spatial distribution of Focal's older sisters as a function of sister's age, x.

1988), and apply time-variant rates (as described above) from the years 1993–2083.

Assuming Focal is born in 1993, the age×stage distributions for Focal's younger sisters as a function of Focal's age are shown in Fig. 8. We see that overall, Focal accumulates more younger sisters than in the time-invariant case (cf. Fig. 5). We also see that Focal retains a larger proportion of these younger sisters, reflected by overall declining mortality rates with time.

To produce an expected age×stage distribution of older sisters, our model accounts for periods by which Focal's mother was reproductive before Focal's birth. We again assume Focal was born in 1993. We see that Focal expects an overall greater amount, and retains a larger proportion, of its expected older sisters; see Fig. 9.

In the next examples, we demonstrate how kin distributions change with time of Focal's birth. For illustrative purposes we consider only younger sisters. Fig. 10 shows the numbers of younger sisters in each specific cluster, for an average Focal born in cluster 3, and whose life-course results in a fixed age-class by 2028, 2063 and 2073. Focal of age-class 25–29 in 2028 will have accumulated a greater number of younger sisters than any other age-class in that period. In periods 2063 and 2073 we see bi-modal shapes describing the number of sisters, as explained by differences in Focals' experiences of demographic rates throughout their lives, namely changes in Total Fertility Rate (TFR).

For a Focal born in cluster 1,3, or 7 and of fixed age-class, Fig. 11 compares the temporal-change in younger sisters which remain in Focal's region of birth to total number of younger sisters. The effects of

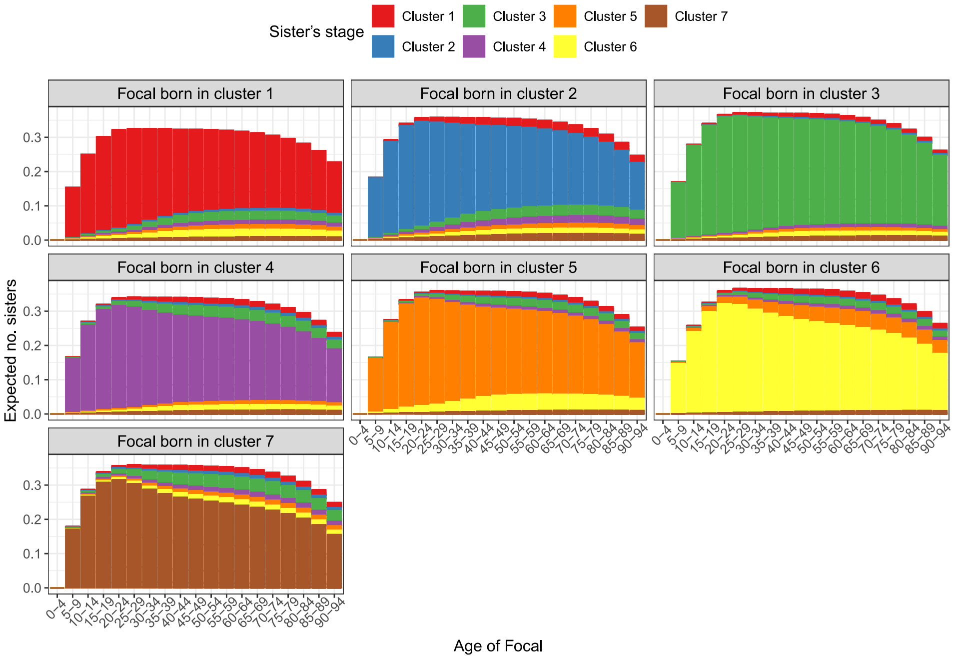

Fig. 8. $g = 1, q = 1$: Spatial distribution of Focal's younger sisters as a function of Focal's age, x, and year. We assume that Focal is born in 1993.

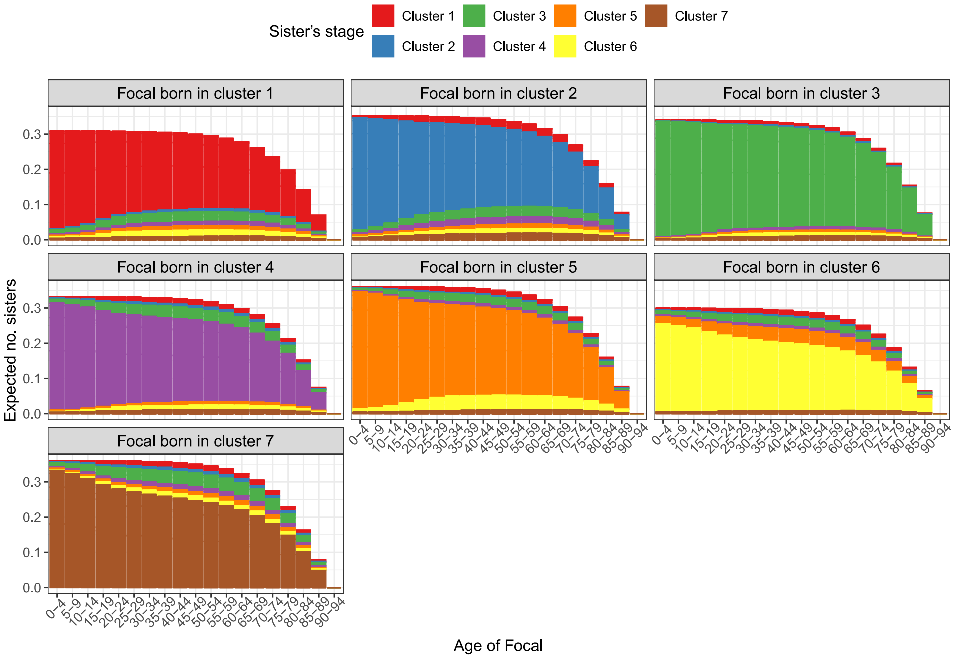

Fig. 9. $g = 1, q = 1$: Spatial distribution of Focal's older sisters as a function of Focal's age, x, and year. We assume that Focal is born in 1993.

ONS future projected decreasing mortality are manifest; the number of alive younger sisters of a Focal in age-class 85–89 increases with time. Focal individuals in age-class 5–9 have nearly all younger sisters within their region of birth. Focal individuals in age-class 85–89 experience a greater number of sisters that have moved; however if Focal is born into cluster 3 we note a relatively smaller number of movers (cf. distributions by stage in Fig. 8). Again assuming Focal is born in cluster 1,3, or 7, the number of younger sisters remaining in Focal's birth region can be visualised as a function of Focal's cohort of birth; see Fig. 12. For a Focal of the 1993 cohort we expect a greater total number of younger sisters (and thus a greater number remaining in Focal's region of birth). We observe a Focal born in 2013 experiences fewer sisters than a Focal born in 2033. This feature is due to TFR decreasing between 2008–2021 but increasing under the ONS projections (from 2022 onwards); Focal born in 2013 gains most younger sisters during 2018 (lower relative TFR) whereas Focal born in 2033 gains most younger sisters in 2038 (higher relative TFR).

4. Discussion

This paper is concerned with kinship networks in time-varying populations described by multiple demographic characteristics. To date, mathematical models of kinship which are not strictly age-structured include the multi-state framework of Caswell (2020) and the class-based framework proposed by Coste et al. (2021). In order to apply the model of Caswell (2020), one requires well-defined initial distributions

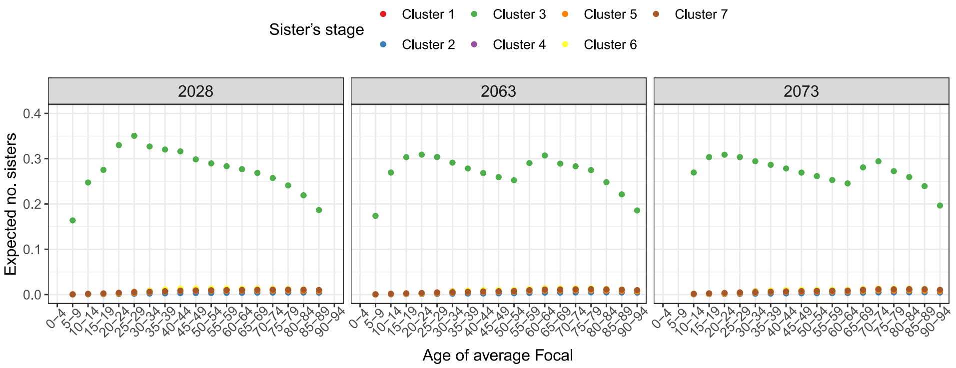

Fig. 10. $g = 1, q = 1$: The number of younger sisters across cluster that an average Focal born in cluster 3 should have accumulated, given life-histories which result in them being of age-class x.

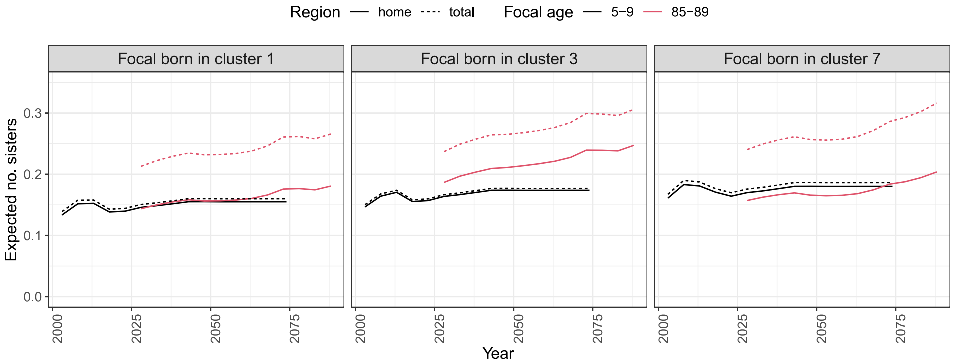

Fig. 11. $g = 1, q = 1$: The number of younger sisters remaining in cluster of Focal's birth compared to total accumulated younger sisters that a Focal of fixed age-class experiences over time.

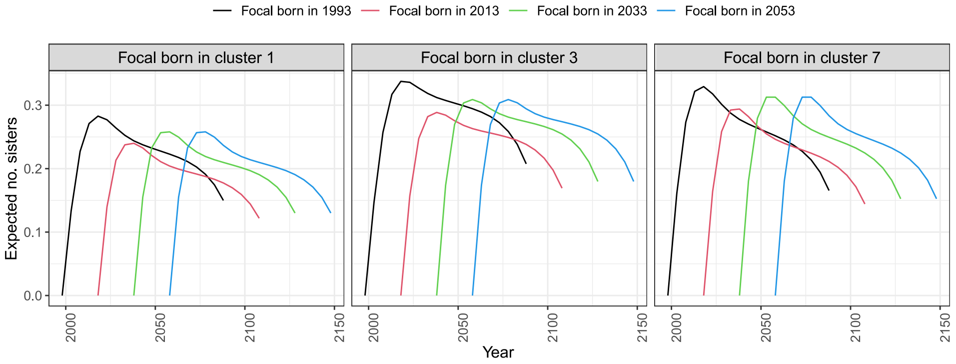

Fig. 12. $g = 1, q = 1$: The number of younger sisters which remain in Focal's cluster of birth, given Focal's cohort of birth.

of kin. In the case whereby kin can move between stage in one direction and at one step per time, the framework is efficient and simple to implement. Otherwise, deriving initial distributions for the dynamic system approach can be non-trivial. To apply the state-of-the-art approach of Coste et al. (2021), one must assume that every individual in Focal's kinship network experiences the same fixed set of demographic rates. This assumption which is rarely satisfied, especially in human populations where for example over the last century fertility rates have been temporally volatile (Berrington et al., 2022). Moreover, the model of that paper does not fully explore the intricacies of age×stage kinship (but see Supplementary material 2.3 (Coste et al., 2021) for a meta-population model). This research remedies the theoretical issues encountered when using the multi-state kinship model of Caswell (2020) by extending the model proposed by Coste et al. (2021). The present work generalises the genealogical Markov approach of counting kin to complex population structures of age and arbitrary stage which change over time.

Many demographic processes cannot simply be explained by age-specific analysis. Additional population characteristic, which we refer to stages, almost invariably affect mortality and fertility schedules. A multi-dimensional view of population processes is therefore important. Within the context of kinship modelling, problems arise due to the diverse and varied nature in which kin can move in and out of stages over their own life-course and over time (Tuljapurkar and Haridas, 2006; Caswell et al., 2018). Kin may move between stages in multiple directions, by multiple step sizes, and at any time during or before a reference Focal individual's life-time. Calculating the stable age×stage distribution of mothers, $\tilde{\boldsymbol{\pi}}$ – a central component to Caswell's (Caswell, 2020) framework – becomes theoretically involved. A model currently in development investigating spatial stage, demonstrates the demands of extending the framework (see Roper and Caswell, 2023). The authors of that paper clarify the difficulties of calculating initial conditions for kin alive before Focal; kin intrinsically conditioned on Focal's stage at birth. The conditioning propagates to each of Focal's ancestors defined through $q > 1$, thereby necessitating a posteriori assumptions to construct an stable age×stage distribution of mothers (cf. Eqs. (24)–(26) in Roper and Caswell, 2023).

The model developed here is beneficial in the sense that the genealogical Markov chains trivially calculate the stable distribution of mothers in the population. To see this, consider a standard time-invariant age-structured population model. One has a projection matrix $\mathbf{A}$, a fertility matrix $\mathbf{F}$ with rows $F_1, F_2, \ldots$, and an associated genealogical reproduction matrix $\mathbf{W}$ defined through the stable population structure $\mathbf{z}$. A randomly selected newborn Focal can be represented by the unit vector $\mathbf{e}_1$. It is simple to derive the equality

$$\left(\mathbf{e}_1^\dagger \mathbf{W}\right)^\dagger = \boldsymbol{\pi} \equiv \mathbf{z} \circ F_1^\dagger. \tag{15}$$

The right hand side of Eq. (15), through the Hadamard product, shows the established method for defining the stable distribution of mothers in the population. This procedure however does not extend naturally to population structures characterised by block-structured fertility matrices $\tilde{\mathbf{F}}$. Indeed, the existing multi-state kinship model simply sums the age×stage offspring of mothers in the population and places newborns into the first stage (see Eq. (14) in Caswell, 2020). Assuming that newborns always begin life in the first stage severely limits the applicability of the model; problems arise when offspring can be born into any stage. In this case, the marginal age-distribution of mothers $\boldsymbol{\pi}$ is no longer valid, and the existing model cannot be applied. A simple example is when stage is defined geographically (Raymer et al., 2019). On the other hand, the genealogical Markov chain naturally derives the stable distribution of mothers in the population, and is valid under any type of stage considered to structure population.

Another feature of Eq. (15) is that it introduces an explicit time dependence. Within our time-variant multi-state framework, $\left(\mathbf{e}_1^\dagger \mathbf{W}\right)^\dagger$ becomes $\left(\tilde{\phi}_0^\dagger \tilde{\mathbf{W}}_{-1}\right)^\dagger$, which by construction, yields Focal's mother's age×stage distribution at time strictly before Focal is in existence. Contrastingly, within the existing framework of Caswell (2020), the stable distribution of mothers is defined during the time-interval of Focal's first age-class. This assumption can in two ways lead to over-estimations of particular kin types. We illustrate using an example of an abridged life table with age grouped by 5 year intervals. First, if the stable distribution of mothers is defined during Focal's first age-class, then Focal's mother must be alive while Focal is aged between 0 and 4 years old. An alive mother is more likely to have offspring than a dead one. Second, rather than projecting sisters which are born in a time-interval strictly after the one in which Focal was born, one actually projects sisters also born during the same time-interval as Focal (here while Focal is 0–4 years old). In order to circumvent such difficulties, we consider a third separate case of kin which descend from same-age-class ancestors (see Appendix A.2). Note that an alternative solution could be to distribute these same-age-class siblings with equal probability into the older/younger categories (Croll and Caswell, 2024). The validity of the assumptions we make here are examined in Appendix D where we compare our theoretical model to a direct stochastic simulation.

Previous models have considered time-invariant age×stage kinship (e.g., Caswell, 2020; Roper and Caswell, 2023; Coste et al., 2021) and are easily recovered by our framework. Here, we extend field to cover the more realistic situation of multi-state kinship depending on changing demographic rates. Time-dependencies in demographic processes have long been recognised (Tuljapurkar and Orzack, 1980; Schreiber and Moore, 2018; Caswell, 2019a) and are crucial to forecasting future population characteristics (Lee and Tuljapurkar, 1994; Alburez-Gutierrez et al., 2023). Although the model presented here treats rates as deterministic, an extension of the current framework could incorporate environmental (rate) uncertainty. Fluctuations in demographic rates are most commonly theoretically investigated in the asymptotic limit (Tuljapurkar and Orzack, 1980; Tuljapurkar, 1982; Giaimo, 2023), whereas the dynamics of Focal's kin operate on a short timescale. Future work within our framework could apply methods similar to the approximations of stochastic forecasts, proposed by Lee & Tuljapurkar (Lee and Tuljapurkar, 1994). This would allow one to forecast populations of kin demarcated by stage. Such progress would be especially useful in human demographics with social/economic/health related stages – for example to project the expected number of kin with disability in the future.

We note several limitations of the model presented herein. Currently our model only considers one sex populations; however a two-sex analogue has also been analysed and is intended for future publication. An important assumption on which our model depends is that each projection matrix $\tilde{\mathbf{A}}_t$ is irreducible. While reducible, the matrix need not exhibit a well defined genealogical decomposition. One can numerically check for the existence of a strictly positive eigenvector, $\tilde{\mathbf{z}}_t$, such that $\tilde{\mathbf{A}}_t \tilde{\mathbf{z}}_t = \lambda(t) \tilde{\mathbf{z}}_t$. It is then well-known (e.g., 8.3.4, Horn and Johnson, 2010) that $\lambda(t) = \rho(\tilde{\mathbf{A}}_t)$, and thus Eq. (3)-Eq. (5) are well defined. Otherwise, while projection matrices are reducible, we explain in Appendix C necessary conditions for $\tilde{\mathbf{z}}_t$ to be positive. If non-positive, we show that by studying the Frobenius Normal form of $\tilde{\mathbf{A}}_t$ and its associated directed graph, one can deduce which entries $\tilde{z}_i(t)$ of $\tilde{\mathbf{z}}_t$ are zero.

From a computational perspective, the summations within our kinship formulae are expensive, and in general, operate over biologically infeasible cases. Once a specific demographic problem is considered however, one can make efficiencies. For instance a closed fertility interval $R_t = [x_a, x_b]$ constrains the cardinalities of $\mathcal{S}_t^q$ and $\mathcal{Q}_{t,x}^g$, thereby reducing the number of operations in Eq. (7) and Eq. (9). The size of the set $\mathcal{Q}_{t,x}^g$ is ${}^{t+x}C_g$ (where C represents the binomial coefficient). If we impose the condition $|s_i - s_j| \in R_t, \forall i, j \in \{1, 2, \ldots, g\}$ then the set size reduces to ${}^{t+x-gx_a+x_a}C_g - {}^{t+x+1-gx_b+x_b}C_g$. In practical terms supposing that $g = 2, t = 19, x = 19, x_a = 4, x_b = 9$, by imposing these constraints we reduce the number of calculations performed from 703 to 126. It terms of longevity, a generation within Focal's family tree can be truncated using $x^* = \inf\{x : \|\!|\Gamma^{\mathcal{V}}(x, -1)\|\!|_1 < \epsilon\}$ for $\epsilon \ll 1$, i.e., to some sufficiently small probability of being alive over x^* years. Therefore the $t-$summations in Eq. (11) and Eq. (A.2) can be approximated to any level of accuracy ϵ, by setting an upper bound of $t \leq qx^*$.

In future work it will be of interest to contrast the complexity required to implement this model to that of a microsimulation. A benefit of simulating is the emergent nature in which kinship networks are formed. One does not need consider the (theoretically) distinct regimes as covered in Section 2.3, Appendix A.1 and Appendix A.2. Instead, kin can be trivially linked by recording lines of ancestry. Simulating also circumvents the need for the restrictive assumptions of population structure (see Eq. (3) and Eq. (5)). Births, deaths, and migration events are random variables, occurring with probabilities at the individual level. As such, population dynamics display inherent fluctuations. While simulating provides a relatively simple way to reproduce such population movement, the matrix approach here is restricted by deterministic equations; individual stochasticity is not incorporated into our modelling framework. Yet the deterministic projection matrices we apply are simply the expectations of stochastic projection models, their entries derived from probability generating functions (PGFs) of multi-type branching processes (Allen, 2010). An open challenge, both from a theoretical and computational viewpoint, is to extend our model to project PGFs of kin distributions as well as expected values (e.g., see Caswell, 2024). A final advantage of simulating over the analytical approach is due to the latter's constraints in dimension, i.e., how many types of stage one wishes to consider. More complex scenarios could be explored through Agent Based Models – e.g., two-sex kinship subject to time-variant rates, and with more than two stages – but not easily by the matrix-based system.

In conclusion, the formal modelling of multi-state kinship needs to be generalised to a comprehensive framework, able to account for arbitrary stage, and free of theoretical constraints. Through an alternative mathematical approach, this work provides steps towards such a comprehensive theory. Although emphasis is placed on human demography above, our model is broad enough to also capture the dynamics of kinship over a wide range of ecological and biological stage-structured populations. In the above research, we extend age×stage kinship to represent any population characteristic, and under realistic cases of time-changing demographic rates. Our study contributes to the existing literature on kinship by providing succinct formulae which yield the distributions for any kin of some random population member.

CRediT authorship contribution statement

Joe W.B. Butterick: Writing – review & editing, Writing – original draft, Methodology, Investigation, Formal analysis, Conceptualization. **Peter W.F. Smith:** Writing – review & editing, Writing – original draft, Investigation. **Jakub Bijak:** Writing – review & editing, Writing – original draft, Investigation. **Jason Hilton:** Writing – review & editing, Writing – original draft, Data curation.

Declaration of competing interest

The authors declare that they have no known competing financial interests or personal relationships that could have appeared to influence the work reported in this paper.

Acknowledgements

We would like to thank Mark Roper and Hal Caswell for valuable discussions and helpful comments on this project, as well as two anonymous reviewers for their constructive feedback on an earlier draft of this work. All authors acknowledge that the research was supported by the Economic and Social Research Council (ESRC) CPC-Connecting Generations Centre (grant ES/W002116/1).

Appendix A. Supplementary data

Supplementary material related to this article can be found online at https://doi.org/10.1016/j.tpb.2025.02.002.

Data availability

Data and code used can be found https://github.com/ButterickJoe/Simulation_Age_Stage_Kinship.

References

Alburez-Gutierrez, D., Williams, I., Caswell, H., 2023. Projections of human kinship for all countries. Proc. Natl. Acad. Sci. 120 (52), e2315722120.

Allen, L.J.S., 2010. An Introduction to Stochastic Processes with Applications to Biology. Chapman and Hall/CRC, New York.

Berrington, A., Ellison, J., Kuang, B., Vasireddy, S., Kulu, H., 2022. Scenario-based fertility projections incorporating impacts of COVID-19. Popul. Space Place 28 (2), e2546.

Bienvenu, F., Akçay, E., Legendre, S., McCandlish, D.M., 2017. The genealogical decomposition of a matrix population model with applications to the aggregation of stages. Theor. Pop. Biol. 115, 69–80.

Caswell, H., 2019a. Sensitivity Analysis: Matrix Methods in Demography and Ecology. Springer Cham, 6330 Cham, Switzerland.

Caswell, H., 2019b. The formal demography of kinship: A matrix formulation. Demogr. Res. 41 (24), 679–712.

Caswell, H., 2020. The formal demography of kinship II: Multistate models, parity, and sibship. Demogr. Res. 42 (38), 1097–1146.

Caswell, H., 2022. The formal demography of kinship IV: Two-sex models and their approximations. Demogr. Res. 47 (13), 359–396.

Caswell, H., 2024. The formal demography of kinship VI: Demographic stochasticity and variance in the kinship network. Demogr. Res. 51 (39), 1201–1256.

Caswell, H., de Vries, C., Hartemink, N., Roth, G., van Daalen, S.F., 2018. Age × stage-classified demographic analysis: a comprehensive approach. Ecol. Monogr. 88 (4), 560–584.

Caswell, H., Song, X., 2021. The formal demography of kinship III: Kinship dynamics with time-varying demographic rates. Demogr. Res. 45 (16), 517–546.

Coresh, J., Goldman, N., 1988. The effect of variability in the fertility schedule on numbers of kin. Math. Popul. Stud. 1 (2), 137–156.

Coste, C.F.D., Bienvenu, F., Ronget, V., Ramirez-Loza, J.-P., Cubaynes, S., Pavard, S., 2021. The kinship matrix: inferring the kinship structure of a population from its demography. Ecol. Lett. 24 (12), 2750–2762.

Croll, J.C., Caswell, H., 2024. Family matters: Linking population growth, kin interactions, and African elephant social groups. Amer. Nat. E000.

Demetrius, L., 1974. Demographic parameters and natural selection. Proc. Natl. Acad. Sci. 71 (12), 4645–4647.

Demetrius, L., 1975. Natural selection and age-structured populations. Genetics 79 (3), 535–544.

Giaimo, S., 2023. On two conjectures about perturbations of the stochastic growth rate. Aust. N. Z. J. Stat. 65 (1), 1–13.

Goldman, N., 1978. Estimating the intrinsic rate of increase of population from the average numbers of younger and older sisters. Demography 15, 499–507.

Goodman, L.A., Keyfitz, N., Pullum, T.W., 1974. Family formation and the frequency of various kinship relationships. Theor. Pop. Biol. 5 (1), 1–27.

Horn, A.R., Johnson, C.R., 2010. Matrix Analysis. Cambridge University Press, Cambrdige, UK.

Lee, R.D., Tuljapurkar, S., 1994. Stochastic population forecasts for the United-States - beyond high, medium, and low. J. Amer. Statist. Assoc. 89 (428), 1175–1189.

Magnus, J.R., Neudecker, H., 2019. Matrix Differential Calculus with Applications in Statistics and Econometrics. John Wiley & Sons, Inc, Chichester.

NOMIS, 2023. Mid-year population exposures by local authority and five-year age, 1993 to 2021, England and Wales. URL https://www.nomisweb.co.uk/query/construct/summary.asp?reset=yes&mode=construct&dataset=31&version=0&anal=1.

ONS, 2023a. Death registrations by five year age group and local authority, 1981 to 2021, England and Wales. URL https://www.ons.gov.uk/peoplepopulationandcommunity/birthsdeathsandmarriages/deaths/adhocs/1219deathregistrationsbysexfiveyearagegroupandlocalauthorityenglandandwales1981to2021.

ONS, 2023b. Internal migration by local authority and region, five-year age group and sex, England and Wales. URL https://www.ons.gov.uk/peoplepopulationandcommunity/populationandmigration/migrationwithintheuk/datasets/internalmigrationmovesbylocalauthoritiesandregionsinenglandandwalesby5yearagegroupandsex.

ONS, 2023c. Live births by age of mother and local authority, 1993 to 2021, England and Wales. URL.

ONS, 2023d. Past and projected mortality rates (q_x) from the 2020-based (England and Wales) life-tables.. URL https://www.ons.gov.uk/peoplepopulationandcommunity/birthsdeathsandmarriages/lifeexpectancies/datasets/mortalityratesqxprincipalprojectionenglandandwales.

ONS, 2023e. Subnational Population Projections: Births by age of mother, mid-2019 to mid-2043. URL.

ONS, 2023f. Subnational Population Projections: Deaths by local authority and five-year of age. URL.

ONS, 2023g. Subnational Population Projections: Exposures by local authority and five-year of age. URL.

Pavard, S., Coste, C.F.D., 2020. Goodman, Keyfitz & Pullum (1974) and the population frequencies of kinship relationships. Theor. Pop. Biol. 133, 15–16.

Pullum, T.W., 1982. The eventual frequencies of kin in a stable population. Demography 19, 549–565.

Raymer, J., Willekens, F., Rogers, A., 2019. Spatial demography: A unifying core and agenda for further research. Popul. Space Place 25 (4), e2179.

Roper, M., Caswell, H., 2023. Kin in Space. University of Amsterdam, in preparation.

Schreiber, S.J., Moore, J.L., 2018. The structured demography of open populations in fluctuating environments. Methods Ecol. Evol. 9 (6), 1569–1580.

Song, X., Mare, R.D., 2019. Shared lifetimes, multigenerational exposure, and educational mobility. Demography 56, 891–916.

Tuljapurkar, S.D., 1982. Population dynamics in variable environments. IV. Weak ergodicity in the Lotka Equation. J. Math. Biol. 14, 221–230.

Tuljapurkar, S., 1993. Entropy and convergence in dynamics and demography. J. Math. Biol. 31, 253–271.

Tuljapurkar, S., Haridas, C.V., 2006. Temporal autocorrelation and stochastic population growth. Ecol. Lett. 9 (3), 327–337.

Tuljapurkar, S.D., Orzack, S.H., 1980. Population dynamics in variable environments. I. Long-run growth-rates and extinction. Theor. Pop. Biol. 18 (3), 314–342.